Romanian Reports in Physics **72**, 405 (2020)

SINE-GORDON BREATHERS AND FORMATION OF EXTREME WAVES IN SELF-INDUCED TRANSPARENCY MEDIA

CHONG HOU[1], LILI BU[1], FABIO BARONIO[2], DUMITRU MIHALACHE[3], SHIHUA CHEN[1,*]

[1]School of Physics, Southeast University, Nanjing 211189, China
[2]INO CNR and Dipartimento di Ingegneria dell'Informazione,
Università di Brescia, Via Branze 38, 25123 Brescia, Italy
[3]Horia Hulubei National Institute for Physics and Nuclear Engineering,
Department of Theoretical Physics, Bucharest-Magurele, RO-077125, Romania
[*]Corresponding author, Email: *cshua@seu.edu.cn*

Received February 7, 2020

Abstract. We investigate the formation of optical extreme waves in a resonant two-level medium that entails the self-induced transparency (SIT) effect, within the framework of the sine-Gordon equation. By virtue of the exact breather solutions and numerical simulations, we reveal that the extreme waves may occur as a result of an intense interaction between individual breather components, by an optimal choice of the breathing periods and the propagation directions for each component. We expect that this work may stimulate the experimental study of the extreme wave formation in SIT media.

Key words: Extreme waves, self-induced transparency, sine-Gordon equation.

1. INTRODUCTION

Nowadays, there is a surge of intense research activities on understanding the underlying physical processes that drive the appearance of extreme wave events in real-world settings [1–10]. This has particularly blossomed in the field of optics and photonics, due to the availability of reliable laser sources and advanced material fabricating and diagnostic technologies [11]. Since the first ever demonstration of optical rogue wave events in the process of soliton-fission supercontinuum generation [12], other physical processes, such as modulation instability [13, 14], integrable turbulence [15], optical filamentation [16], soliton or breather collisions [17], and even the linear asymmetry and inhomogeneity [18, 19], were also known for generating extreme waves. Of particular interest is the multiple soliton and breather interaction case, where the governing models can be of real-field characteristic, like the modified Korteweg–de Vries equation [17] and the Kadomtsev–Petviashvili equation [20–22], among others. These real-field integrable models may not involve any complex rational solutions (*e.g.*, the Peregrine soliton solutions [23–29]) often met in the study of rogue waves, but still allow the generation of huge strongly localized transient waves via a complex multiple soliton collision process.

In this paper, we wish to uncover the similar extreme wave dynamics in self-induced transparency (SIT) media, within the framework of sine-Gordon equation, which is also a popular real-field integrable model [30]. Actually, in the past decades, the sine-Gordon model has found significant applications in diverse areas such as differential geometry, Josephson junctions, solid-state physics, field theory, and ultrafast optics [31]. Particularly, in optical contexts, this model or its generalization has been widely used to describe the SIT effect in a resonant two-level medium [32, 33], the formation of few-cycle solitons in the short-wave approximation regime [34], the supercontinuum generation in gas-filled hollow waveguides [35, 36], the existence of stable light bullets in bulk SIT media [37], the topological solitons as addressable phase bits in a driven laser [38], the high harmonic generation in the attosecond regime [39], and the stable propagation of 3D bipolar ultrashort pulses in arrays of carbon nanotubes [40, 41]. However, the multiple breather collision process of this model, with a special application to the SIT media for understanding the extreme wave formation, was not well studied before, to the best of our knowledge.

In the following, we shall start our analysis with the underlying physics responsible for the SIT phenomenon. We will demonstrate, both analytically and numerically, that the extreme waves may occur as a result of an intense interaction between individual breather components, by an optimal choice of the breathing periods and the propagation directions for each component. We expect that our work may stimulate the experimental study of the extreme wave formation in SIT media.

The structure of this paper is organized as follows. In Sec. 2, the SIT phenomenon is briefly discussed, the sine-Gordon model is introduced and its general multiple-breather solutions are obtained by using the Darboux dressing method. The formation of extreme waves in SIT media is investigated in Sec. 3 by using the exact multiple-breather solutions and numerical simulations. Finally, in Sec. 4 we summarize the obtained results.

2. SELF-INDUCED TRANSPARENCY, SINE-GORDON MODEL, AND GENERAL MULTIPLE-BREATHER SOLUTIONS

As is well known, the interaction of optical pulses with nonlinear resonant media enjoys a special status in atomic and nonlinear optics [42, 43]. When such interaction occurs on a time-scale faster than the characteristic (polarization and inversion) relaxation times of the resonant medium, an SIT phenomenon may appear [32], in a way that the leading edge of the incident pulse inverts the population of a cold atomic ensemble, while the trailing edge returns the population to its initial state by a stimulated emission process [33]. As a result, a steady soliton-like pulse is established in an otherwise absorbing medium, maintaining a fixed pulse area, but with a velocity three orders of magnitude less than the phase velocity of light, c, in

the medium.

Basically, the theory of the interaction of radiation with an ensemble of two-level atoms is constituted by the optical Bloch equations for atoms and the Maxwell's equations for the classical electromagnetic field. In the slowly varying envelope and phase approximation, and assuming a sharp-line lineshape, such interaction can be governed by the system of SIT equations [33, 42]:

$$\left(\frac{\partial}{\partial t}+c\frac{\partial}{\partial z}\right)A=\kappa P, \tag{1}$$

$$\frac{\partial Q}{\partial t}=\Delta\omega P, \quad \frac{\partial P}{\partial t}=-\Delta\omega Q+\kappa AR, \quad \frac{\partial R}{\partial t}=-\kappa AP, \tag{2}$$

where $A(z,t)$ is the normalized amplitude of the optical field that has the form

$$E(z,t)=\frac{\hbar\kappa}{d}A(z,t)\cos[\omega_0(t-z/c)-\theta(z,t)],$$

$\theta(z,t)$ is a slowly-varying phase, $\hbar$ is the Planck's constant divided by 2π, $\kappa=(2\pi n_0\omega_0 d^2/\hbar)^{1/2}$ is a constant associated to the Rabi frequency $\omega_R=\kappa A$, ω_0 is the carrier frequency, $\Delta\omega=\omega-\omega_0$ is the detuning of the resonant transition frequency ω from ω_0, n_0 is the density of active atoms, d is the atomic dipole matrix element, P and Q are the quadrature components of the atomic polarization, and R is the population difference of two atomic states. It follows easily from Eqs. (2) that

$$P^2+Q^2+R^2=1, \tag{3}$$

which indicates that the tip of the Bloch vector (P,Q,R) traces out a path on the Bloch sphere of unit radius.

Naturally, once a perfect resonance is met (*i.e.*, $\Delta\omega=0$), one can obtain from Eqs. (2) $Q=0$, and then from Eq. (3) that $P=-\sin[u(z,t)]$ and $R=-\cos[u(z,t)]$, where $u(z,t)$ can be defined as the rotation angle of the Bloch vector in the PR plane, relating to the optical field by an integral expression:

$$u(z,t)=\kappa\int_{-\infty}^{t}A(z,t)dt. \tag{4}$$

Then, by change of variables, the SIT equations (1) and (2) can boil down to the celebrated sine-Gordon equation:

$$\frac{\partial^2 u(\xi,\tau)}{\partial\xi\partial\tau}=-\sin\left[u(\xi,\tau)\right], \tag{5}$$

where $\xi=\kappa z/c$ is the normalized distance, and $\tau=\kappa(t-z/c)$ is the normalized retarded time. The minus sign on the right-hand side of Eq. (5) indicates that the medium where the pulse propagates is ordinarily absorbing, *i.e.*, an attenuator. In

terms of the new variables, the pulse amplitude can be expressed as

$$A = \frac{1}{\kappa}\frac{\partial u}{\partial t} = \frac{\partial u}{\partial \tau}. \tag{6}$$

Therefore, if an SIT effect occurs in such a resonant medium, the pulse area σ can be simply equal to the difference between the rotation angles at positive and negative infinities, namely,

$$\sigma = \kappa \int_{-\infty}^{\infty} A(z,t)dt = u(\xi,+\infty) - u(\xi,-\infty). \tag{7}$$

The sine-Gordon equation (5) had received great popularity in the 1970s as a result of the discovery of its integrability and development of the understanding of the significance of this equation as a model of many important physical systems [31]. As early as that period, many exact solutions of this model, including those called kinks, solitons, and breathers, have been established, by means of the inverse scattering transform, the Bäcklund transform, or the Hirota bilinear method [44–46].

Here, we are particularly concerned with the breather solutions, which in fact involve more plenteous dynamics than might be expected. By virtue of the Darboux dressing method [47, 48], we obtain the exact general nth-order breather solution:

$$u^{[n]} = 4\arctan\left(\frac{\mathrm{i}\{\det[(B_{ij})_{2n\times 2n}] - \det[(C_{ij})_{2n\times 2n}]\}}{\det[(B_{ij})_{2n\times 2n}] + \det[(C_{ij})_{2n\times 2n}]}\right), \tag{8}$$

where '$\det$' means taking the determinant of the matrix and B_{ij} and C_{ij} are the matrix elements specified by

$$B_{ij} = \mu_j^{i-1}(\mathrm{i}m_j + (-1)^{i-1}), \tag{9}$$

$$C_{ij} = \mu_j^{i-1}(\mathrm{i}m_j - (-1)^{i-1}), \tag{10}$$

where $\mu_j = \alpha_k e^{\mathrm{i}\theta_k}$, $m_j = \exp(T_k + \mathrm{i}X_k)$ if $j = 2k-1$, and $\mu_j = \alpha_k e^{-\mathrm{i}\theta_k}$, $m_j = \exp(T_k - \mathrm{i}X_k)$ if $j = 2k$, for $k = 1, 2, \cdots, n$. Here the functions X_k and T_k are defined as below, through the real constants θ_k, α_k, β_k, and γ_k,

$$X_k = \sin(\theta_k)(\alpha_k\tau + \xi/\alpha_k) + \beta_k, \tag{11}$$

$$T_k = \cos(\theta_k)(\alpha_k\tau - \xi/\alpha_k) + \gamma_k. \tag{12}$$

Hence, the nth-order breather given by Eq. (8) involves $4n$ free parameters and is thus of the most general form. Below, one may assume $0 < \theta_k < \pi/2$, without loss of generality. As an example, by letting $n = 1$ in Eq. (8), the first-order breather reads as $u(\xi,\tau) = 4\arctan[\cot(\theta_1)\sin(X_1)\mathrm{sech}(T_1)]$, which possesses 4 real parameters θ_1, α_1, β_1, and γ_1. It can be considered as a kink-antikink bound state, featuring a breathing frequency by $\sin(\theta_1)$ and an energy proportional to $\cos(\theta_1)$ [31]. On the

other side, in the small-amplitude limit, *i.e.*, as $\theta_1 \to \pi/2$, this first-order breather can approximately take the form $u(\xi,\tau) \approx 4(\pi/2-\theta_1)\sin(X_1)\mathrm{sech}(T_1)$, which is tantamount to the fundamental soliton of the nonlinear Schrödinger equation [49].

3. EXTREME WAVE FORMATION AND NUMERICAL SIMULATIONS

We will show that, for higher-order breathers, these free parameters each play an intriguing role in determining the breather dynamics. Let us illustrate this with the second-order breather ($n = 2$), which takes the following explicit form

$$u(\xi,\tau) = 4\arctan\left(\frac{H}{D}\right), \tag{13}$$

where

$$\begin{aligned} H = {} & \frac{\left[\cos^2(\theta_1)-\cos^2(\theta_2)+\frac{(\alpha_1^2-\alpha_2^2)^2}{4\alpha_1^2\alpha_2^2}\right]\sin(X_1)\cosh(T_2)}{\sin(\theta_1)\cos(\theta_2)} \\ & + \frac{\left[\sin^2(\theta_1)-\sin^2(\theta_2)+\frac{(\alpha_1^2-\alpha_2^2)^2}{4\alpha_1^2\alpha_2^2}\right]\sin(X_2)\cosh(T_1)}{\cos(\theta_1)\sin(\theta_2)} \\ & + \frac{\alpha_1^2-\alpha_2^2}{\alpha_1\alpha_2}\left[\cos(X_1)\sinh(T_2)-\cos(X_2)\sinh(T_1)\right], \end{aligned} \tag{14}$$

$$\begin{aligned} D = {} & \frac{\left[\cos^2(\theta_1)+\cos^2(\theta_2)+\frac{(\alpha_1^2-\alpha_2^2)^2}{4\alpha_1^2\alpha_2^2}\right]\cosh(T_1)\cosh(T_2)}{\cos(\theta_1)\cos(\theta_2)} \\ & - \frac{\left[\sin^2(\theta_1)+\sin^2(\theta_2)+\frac{(\alpha_1^2-\alpha_2^2)^2}{4\alpha_1^2\alpha_2^2}\right]\sin(X_1)\sin(X_2)}{\sin(\theta_1)\sin(\theta_2)} \\ & - \frac{\alpha_1^2+\alpha_2^2}{\alpha_1\alpha_2}\left[\cos(X_1)\cos(X_2)+\sinh(T_1)\sinh(T_2)\right]. \end{aligned} \tag{15}$$

It is obvious that this general breather solution involves eight free parameters $\theta_{1,2}$, $\alpha_{1,2}$, $\beta_{1,2}$, and $\gamma_{1,2}$, and may thus bring about many novel dynamics. So is the case with the evolution of the optical field A, which is given by

$$A = \frac{\partial u}{\partial \tau} = \frac{4(D\partial H/\partial\tau - H\partial D/\partial\tau)}{H^2+D^2}. \tag{16}$$

Figure 1 shows the evolutions of the second-order breather state, which consists of two fundamental sine-Gordon breathers, for both the rotation angle u (left column) and the optical field A (right column), using different sets of free parameters that have been specified in the caption. On the rotation angle side, one can find that each breather component u_j ($j = 1, 2$) will generally have a nonlinear velocity given

by $d\tau/d\xi = 1/\alpha_j^2$, a peak amplitude given by $4(\pi/2 - \theta_j)$, a breathing frequency denoted by $\sin(\theta_j)$, a longitudinal translation determined by β_j, and a transversal translation by γ_j. Accordingly, in Fig. 1(a), one can see that the first sine-Gordon breather on the left side involves a peak amplitude $3\pi/2$, with a larger oscillating period, while the second one on the right side will have a peak amplitude π, with a smaller oscillating period, both of which propagate along the same direction and are thus well separated with an interval determined by γ_j. More interestingly, by an appropriate choice of the values of parameters $\beta_{1,2}$, the two sine-Gordon breathers of different α_j values will collide and the maximum peak amplitude occurs in the interaction center, which can be as high as $4(\pi - \theta_1 - \theta_2)$; for example, in Figs. 1(c) and 1(e), the maximum peak amplitude will reach the values $5\pi/2$ and $14\pi/5$, respectively, for the specific parameters used.

However, on the optical field side, it may appear different dynamics, as the optical field A is the time derivative of the rotation angle u. Figures 1(b), 1(d), and 1(f) demonstrate the corresponding evolutions of optical field A under the same parameter conditions as used in the left column. It is clear that the optical field components also exhibit the breather dynamics determined by the parameters θ_j and a different propagation direction determined by α_j, while with the longitudinal and transversal translations determined by β_j and γ_j, respectively. More strikingly, one can see in Fig. 1(f) that there appears an extreme wave in the interaction regime, which is much higher in peak amplitude than the surrounding waves, analogous to the formation of rogue wave events in optical media [50, 51].

In order to reveal this interesting extreme-wave dynamics, we consider the interaction of two sine-Gordon breathers of different propagation directions, as shown in Fig. 2, where we use the parameters $\theta_1 = \theta_2 = \pi/8$, $\alpha_1 = 5/4$, $\alpha_2 = 2$, and $\gamma_1 = \gamma_2 = 0$. In Figs. 2(a) and 2(b), we show that the peak amplitude in the interaction center for the rotation angle u reaches its maximum (minimum) at $\beta_1 = \beta_2 = \pi/2$ $(-\pi/2)$, whereas the peak amplitude for the optical field A will become zero, as indicated in Figs. 1(c) and 1(d). However, when $\beta_1 = \beta_2 = 0$, the rotation angle u has the largest slope in the interaction center, and the optical field A will soar on the same point, with the peak amplitude much higher than those of the surrounding waves, as seen in Figs. 2(c) and 2(d). This is more evident in Figs. 2(e) and 2(f), where the profiles of the rotation angle and the optical field are plotted at the input ($\xi = -25$) and at the collision center ($\xi = 0$), respectively. As one can see from Fig. 2(f), the optical pulse always features the 0π pulse area [42], and it will undergo a drastic compression in the interaction center, leading to the formation of strongly localized transient extreme waves.

Now a natural question arises: would this train of 0π breather pulses be stable enough to propagate? To this end, we perform the numerical simulations of the equivalent of the sine-Gordon equation (5) in the new system of coordinates $X =$

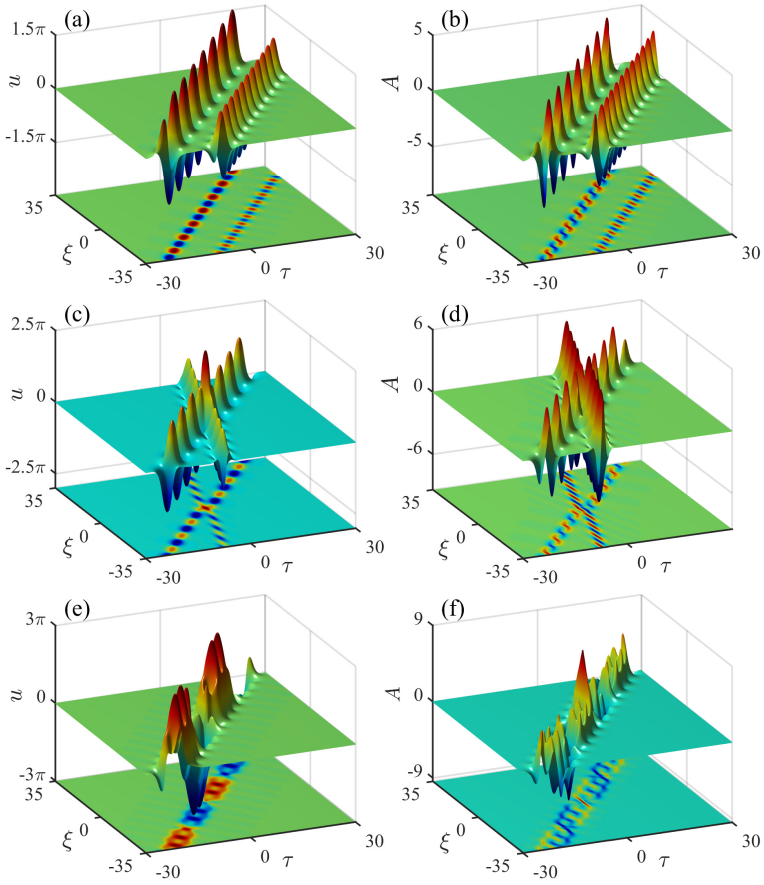

Fig. 1 – Surface (top) and contour (bottom) plots showing the interactions between two sine-Gordon breathers. (a), (c), (e): the evolutions of the rotation angle u, with each component having a fixed amplitude of $4(\pi/2-\theta_j)$ $(j=1,2)$. (b), (d), (f): the corresponding evolutions of the optical field $A=\partial u/\partial\tau$. The specific parameters are given by (a), (b): $\theta_1=\pi/8$, $\theta_2=\pi/4$, $\alpha_1=\alpha_2=5/4$, $\gamma_2=-10$; (c), (d): $\theta_1=\pi/8$, $\theta_2=\pi/4$, $\alpha_1=5/4$, $\alpha_2=2$, $\beta_1=\beta_2=\pi/2$; and (e), (f): $\theta_1=\pi/20$, $\theta_2=\pi/4$, $\alpha_1=\alpha_2=5/4$. Other parameters are set to zero.

$\alpha_1\tau+\xi/\alpha_1$ and $T=\alpha_1\tau-\xi/\alpha_1$ that is comoving with the first breather:

$$\frac{\partial u}{\partial X}=v,\quad \frac{\partial v}{\partial X}-\frac{\partial^2 u}{\partial T^2}+\sin(u)=0, \tag{17}$$

using an efficient code based on the Fourier pseudospectral method [52]. To show the stability, we put the white noise onto the initial profile by multiplying $u(X=-15,T)$ and its spatial derivative $v(X=-15,T)$ by the factor $[1+\varepsilon r_i(T)]$ $(i=u,v)$, respectively, where $r_{u,v}$ are two uncorrelated random functions uniformly distributed in the interval $[-1,1]$ and ε is a small parameter defining the noise level. Typical

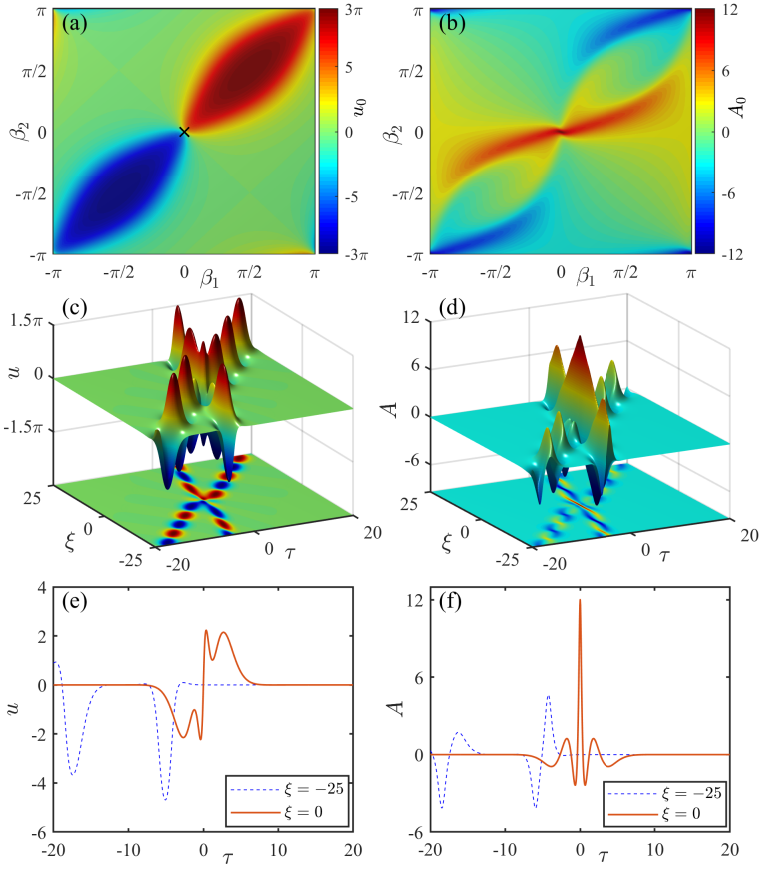

Fig. 2 – Extreme wave arising from the resonant interaction of two sine-Gordon breathers, for given parameters $\theta_1 = \theta_2 = \pi/8$, $\alpha_1 = 5/4$, $\alpha_2 = 2$, and $\gamma_1 = \gamma_2 = 0$. (a) and (b) show, respectively, the phase diagrams of the central amplitudes $u_0 = u(0,0)$ and $A_0 = A(0,0)$ versus β_1 and β_2; (c) shows the evolution of the rotation angle u corresponding to the black cross in (a), *i.e.*, at $\beta_1 = \beta_2 = 0$; (d) plots the corresponding evolution of the optical field $A = \partial u/\partial\tau$; (e) and (f) display the profiles of the rotation angle u and the optical field A at the input and at the collision center, respectively.

results are shown in Figs. 3(a) and 3(b), corresponding to $\varepsilon = 0$ (no noise) and $\varepsilon = 10^{-3}$ (weak noise perturbation), respectively. The other parameters are kept the same as in Fig. 2(c). It is clear that our numerical results, in both the unperturbed and perturbed cases, are well consistent with the analytical ones, as indicated in Fig. 3(c). This suggests that the second-order breather state of 0π pulse area is robust against white-noise perturbation, as did by the 2π sech pulse often seen in SIT media [42].

The role of multiple breather collisions in the generation of extreme waves can be further highlighted by considering the even higher-order sine-Gordon solution

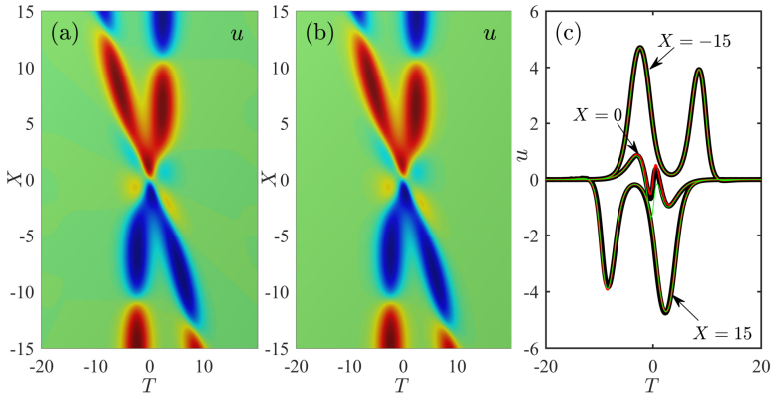

Fig. 3 – Numerical simulation of the evolutions of the rotation angle u for the same free parameters as used in Fig. 2(c), but given in a frame comoving with the first breather, *i.e.*, $X = \alpha_1\tau + \xi/\alpha_1$ and $T = \alpha_1\tau - \xi/\alpha_1$: (a) the unperturbed case ($\varepsilon = 0$); (b) the weak white-noise perturbation case ($\varepsilon = 10^{-3}$). The panel (c) shows the comparison between the numerical profiles (red curves for the $\varepsilon = 0$ case and green ones for the $\varepsilon = 10^{-3}$ case) at $X = -15$, 0, and 15 and their corresponding analytical profiles (black curves).

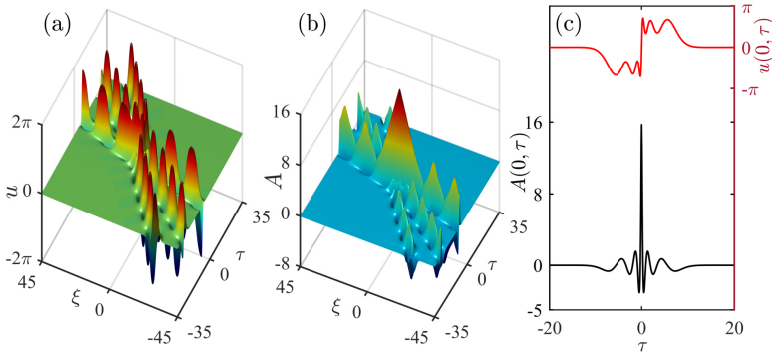

Fig. 4 – Extreme-wave formation due to the interaction between three sine-Gordon breathers, defined by Eq. (8) with $n = 3$, $\alpha_3 = 1$, $\theta_3 = \pi/8$, $\beta_3 = \gamma_3 = 0$, and other parameters being the same as in Figs. 2(c) and 2(d). (a) Rotation angle u; (b) Optical field A; (c) Analytical profiles for the rotation angle $u(0,\tau)$ (red curve) and the optical field $A(0,\tau)$ (black curve).

(8) ($n \geqslant 3$). For example, when three sine-Gordon breathers interact under optimal parameter conditions ($\beta_k = 0$), the extreme-wave amplitude formed will be higher than it would be in the two-breather interaction situation, as indicated in Fig. 4, where the third breather ($\alpha_3 = 1, \theta_3 = \pi/8$) is also put into the two-breather interaction presented in Fig. 2(c). Generally, the peak amplitude of the extreme wave formed will be sum of that of each breather components, and the more breathers get involved in, the higher hump will form, as suggested in Refs. [17, 21].

4. CONCLUSION

In summary, we studied the formation of extreme waves in SIT media, within the framework of the sine-Gordon equation. In terms of the exact explicit second-order breather solution, we demonstrated rich breather dynamics and showed that the extreme waves may form as a result of an intense interaction between individual breather components, by an optimal choice of the breathing periods and propagation directions for each component. We also confirmed our analytical predictions by numerical simulations. We expect that this work will stimulate the experimental study of extreme wave formation in SIT media or in other similar optical settings.

Acknowledgements. This work was supported by the National Natural Science Foundation of China (Grants No. 11974075 and No. 11474051).

REFERENCES

1. J. M. Dudley, F. Dias, M. Erkintalo, and G. Genty, *Instabilities, breathers and rogue waves in optics*, Nature Photon. **8**, 755 (2014).
2. M. Onorato, S. Residori, U. Bortolozzo, A. Montina, and F. T. Arecchi, *Rogue waves and their generating mechanisms in different physical contexts*, Phys. Rep. **528**, 47 (2013).
3. N. Akhmediev *et al.*, *Roadmap on optical rogue waves and extreme events*, J. Opt. **18**, 063001 (2016).
4. S. Wabnitz (ed.), *Nonlinear Guided Wave Optics: A testbed for extreme waves* (IOP Publishing, Bristol, 2017).
5. E. G. Charalampidis, J. Cuevas-Maraver, D. J. Frantzeskakis, and P. G. Kevrekidis, *Rogue waves in ultracold bosonic seas*, Rom. Rep. Phys. **70**, 504 (2018).
6. G. Dematteis, T. Grafke, M. Onorato, and E. Vanden-Eijnden, *Experimental evidence of hydrodynamic instantons: The universal route to rogue waves*, Phys. Rev. X **9**, 041057 (2019).
7. J. M. Dudley, G. Genty, A. Mussot, A. Chabchoub, and F. Dias, *Rogue waves and analogies in optics and oceanography*, Nat. Rev. Phys. **1**, 675 (2019).
8. B. A. Malomed and D. Mihalache, *Nonlinear waves in optical and matter-wave media: A topical survey of recent theoretical and experimental results*, Rom. J. Phys. **64**, 106 (2019).
9. C. B. Ward and P. G. Kevrekidis, *Rogue waves as self-similar solutions on a background: A direct calculation*, Rom. J. Phys. **64**, 112 (2019).
10. N. Akhtar *et al.*, *On the dynamics of dust-acoustic and dust-cyclotron freak waves in a magnetized dusty plasma*, Rom. Rep. Phys. **71**, 403 (2019).
11. M. Närhi, B. Wetzel, C. Billet, S. Toenger, T. Sylvestre, J.-M. Merolla, R. Morandotti, F. Dias, G. Genty, and J. M. Dudley, *Real-time measurements of spontaneous breathers and rogue wave events in optical fibre modulation instability*, Nature Commun. 7, 13675 (2016).
12. D. R. Solli, C. Ropers, P. Koonath, and B. Jalali, *Optical rogue waves*, Nature (London) **450**, 1054 (2007).
13. S. Chen, F. Baronio, J. M. Soto-Crespo, Ph. Grelu, and D. Mihalache, *Versatile rogue waves in scalar, vector, and multidimensional nonlinear systems*, J. Phys. A: Math. Theor. **50**, 463001 (2017).
14. F. Baronio, S. Chen, Ph. Grelu, S. Wabnitz, and M. Conforti, *Baseband modulation instability as*

the origin of rogue waves, Phys. Rev. A **91**, 033804 (2015).
15. J. M. Soto-Crespo, N. Devine, and N. Akhmediev, *Integrable Turbulence and Rogue Waves: Breathers or Solitons?*, Phys. Rev. Lett. **116**, 103901 (2016).
16. S. Birkholz, E. T. J. Nibbering, C. Bree, S. Skupin, A. Demircan, G. Genty, and G. Steinmeyer, *Spatiotemporal rogue events in optical multiple filamentation*, Phys. Rev. Lett. **111**, 243903 (2013).
17. A. V. Slunyaev and E. N. Pelinovsky, *Role of Multiple Soliton Interactions in the Generation of Rogue Waves: The Modified Korteweg–de Vries Framework*, Phys. Rev. Lett. **117**, 214501 (2016).
18. R. Höhmann, U. Kuhl, H. J. Stöckmann, L. Kaplan, and E. J. Heller, *Freak waves in the linear regime: A microwave study*, Phys. Rev. Lett. **104**, 093901 (2010).
19. F. T. Arecchi, U. Bortolozzo, A. Montina, and S. Residori, *Granularity and Inhomogeneity Are the Joint Generators of Optical Rogue Waves*, Phys. Rev. Lett. **106**, 153901 (2011).
20. S. Chen, Ph. Grelu, D. Mihalache, and F. Baronio, *Families of rational soliton solutions of the Kadomtsev–Petviashvili I equation*, Rom. Rep. Phys. **68**, 1407 (2016).
21. S. Chen, Y. Zhou, F. Baronio, and D. Mihalache, *Special types of elastic resonant soliton solutions of the Kadomtsev–Petviashvili II equation*, Rom. Rep. Phys. **70**, 102 (2018).
22. L. Kaur and A. M. Wazwaz, *Bright-dark lump wave solutions for a new form of the (3+1)-dimensional BKP-Boussinesq equation*, Rom. Rep. Phys. **71**, 102 (2019).
23. D. H. Peregrine, *Water waves, nonlinear Schrödinger equations and their solutions*, J. Aust. Math. Soc. B Appl. Math. **25**, 16 (1983).
24. B. Kibler, J. Fatome, C. Finot, G. Millot, F. Dias, G. Genty, N. Akhmediev, and J. M. Dudley, *The Peregrine soliton in nonlinear fibre optics*, Nature Phys. **6**, 790 (2010).
25. G. Yang, Y. Wang, Z. Qin, B. A. Malomed, D. Mihalache, and L. Li, *Breatherlike solitons extracted from the Peregrine rogue wave*, Phys. Rev. E **90**, 062909 (2014).
26. S. Chen, F. Baronio, J. M. Soto-Crespo, Y. Liu, and Ph. Grelu, *Chirped Peregrine solitons in a class of cubic-quintic nonlinear Schrödinger equations*, Phys. Rev. E **93**, 062202 (2016).
27. S. Chen, Y. Ye, J. M. Soto-Crespo, Ph. Grelu, and F. Baronio, *Peregrine Solitons Beyond the Threefold Limit and Their Two-Soliton Interactions*, Phys. Rev. Lett. **121**, 104101 (2018).
28. C.-C. Pan, F. Baronio, and S.-H. Chen, *Recent developments of extreme wave events in integrable resonant systems*, Acta Physica Sinica **69**, 010504 (2020).
29. F. Baronio, S. Chen, and S. Trillo, *Resonant radiation from Peregrine solitons*, Opt. Lett. **45**, 427 (2020).
30. J. Weiss, *The sine-Gordon equations: Complete and partial integrability*, J. Math. Phys. **25**, 2226 (1984).
31. J. Cuevas-Maraver, P. G. Kevrekidis, and F. Williams (eds.), *The sine-Gordon Model and its Applications* (Springer, Cham, 2014).
32. S. L. McCall and E. L. Hahn, *Self-induced transparency by pulsed coherent light*, Phys. Rev. Lett. **18**, 908 (1967).
33. A. I. Maimistov, A. M. Basharov, S. O. Elyutin, and Yu. M. Sklyarov, *Present state of self-induced transparency theory*, Phys. Rep. **191**, 1 (1990).
34. H. Leblond and D. Mihalache, *Models of few optical cycle solitons beyond the slowly varying envelope approximation*, Phys. Rep. **523**, 61 (2013).
35. H. Leblond, Ph. Grelu, and D. Mihalache, *Models for supercontinuum generation beyond the slowly-varying-envelope approximation*, Phys. Rev. A **90**, 053816 (2014).
36. H. Leblond, Ph. Grelu, D. Mihalache, and H. Triki, *Few-cycle solitons in supercontinuum generation dynamics*, Eur. Phys. J. Special Topics **225**, 2435 (2016).
37. M. Blaauboer, B. A. Malomed, and G. Kurizki, *Spatiotemporally Localized Multidimensional Solitons in Self-Induced Transparency Media*, Phys. Rev. Lett. **84**, 1906 (2000).

38. B. Garbin, J. Javaloyes, G. Tissoni, and S. Barland, *Topological solitons as addressable phase bits in a driven laser*, Nat. Commun. **6**, 5915 (2015).
39. A. Nazarkin, *Nonlinear Optics of Intense Attosecond Light Pulses*, Phys. Rev. Lett. **97**, 163904 (2006).
40. A. V. Zhukov, R. Bouffanais, B. A. Malomed, H. Leblond, D. Mihalache, E. G. Fedorov, N. N. Rosanov, and M. B. Belonenko, *Collisions of three-dimensional bipolar optical solitons in an array of carbon nanotubes*, Phys. Rev. A **94**, 053823 (2016).
41. E. G. Fedorov, A. V. Zhukov, R. Bouffanais, B. A. Malomed, H. Leblond, D. Mihalache, N. N. Rosanov, M. B. Belonenko, and T. F. George, *Asymptotic dynamics of three-dimensional bipolar ultrashort electromagnetic pulses in an array of semiconductor carbon nanotubes*, Opt. Express **27**, 27592 (2019).
42. G. L. Lamb, *Analytical Descriptions of Ultrashort Optical Pulse Propagation in a Resonant Medium*, Rev. Mod. Phys. **43**, 99 (1971).
43. L. Allen and J. H. Eberly, *Optical Resonance and Two-Level Atoms* (Wiley, 1975).
44. R. Hirota, *Exact Solution of the Sine-Gordon Equation for Multiple Collisions of Solitons*, J. Phys. Soc. Japan **33**,1459 (1972).
45. M. J. Ablowitz, D. J. Kaup, A. C. Newell, and H. Segur, *Method for Solving the Sine-Gordon Equation*, Phys. Rev. Lett. **30**, 1262 (1973).
46. P. J. Caudrey, J. D. Gibbon, J. C. Eilbeck, and R. K. Bullough, *Exact Multisoliton Solutions of the Self-Induced Transparency and Sine-Gordon Equations*, Phys. Rev. Lett. **30**, 237 (1973).
47. V. A. Andreev and Yu. V. Brezhnev, *Darboux transformation, positons and general superposition formula for the sine-Gordon equation*, Phys. Lett. A **207**, 58 (1995).
48. J. Cen, F. Correa, and A. Fring, *Degenerate multi-solitons in the sine-Gordon equation*, J. Phys. A: Math. Theor. **50**, 435201 (2017).
49. P. Kirrmann, G. Schneider, and A. Mielke, *The validity of modulation equations for extended systems with cubic nonlinearities*, Proc. R. Soc. Edinb. Sect. A-Math. **122**, 85 (1992).
50. S. Chen, X.-M. Cai, Ph. Grelu, J. M. Soto-Crespo, S. Wabnitz, and F. Baronio, *Complementary optical rogue waves in parametric three-wave mixing*, Opt. Express **24**, 5886 (2016).
51. S. Chen, Y. Ye, F. Baronio, Y. Liu, X.-M. Cai, and Ph. Grelu, *Optical Peregrine rogue waves of self-induced transparency in a resonant erbium-doped fiber*, Opt. Express **25**, 29687 (2017).
52. J. A. C. Weideman and S. C. Reddy, *A MATLAB differentiation matrix suite*, ACM T. Math. Software **26**, 465 (2000).